Microwave-Assisted Synthesis of Calcium Carbonate (Vaterite) of Various Morphologies in Water−Ethylene Glycol Mixed Solvents

Rui-Juan Qi and Ying-Jie Zhu*

State Key Laboratory of High Performance Ceramics and Superfine Microstructure, Shanghai Institute of Ceramics, Chinese Academy of Sciences, Shanghai 200050, P.R. China and Graduate School of the Chinese Academy of Sciences, P. R. China

Received: February 13, 2006; In Final Form: March 13, 2006

A fast microwave-assisted method is reported for the synthesis of $CaCO_3$ (vaterite) with various morphologies in the water/ethylene glycol **(**EG) system with surfactants. Our experiments show that microwave heating, reaction time, surfactant, and the water−EG mixed solvents play important roles in the morphology of vaterite. Vaterite with dagger-like, bicone-like, shuttle-like morphology and microspheres self-assembled from nanoparticles have been obtained by adjusting the experimental parameters. The products were characterized by X-ray powder diffraction, transmission electron microscopy, and scanning electron microscopy.

Introduction

Calcium carbonate ($CaCO_3$) is an attractive model mineral for studies in the laboratory because the morphology control of $CaCO_3$ has been an important subject in biomineralization processes.[1,2] $CaCO_3$ can crystallize as calcite, aragonite, and vaterite. Calcite and aragonite are the most common biologically formed $CaCO_3$ polymorphs. Vaterite, a less stable polymorph, will transform into calcite via a solvent-mediated process.[3] However, vaterite is expected to have potential applications for various purposes because it has features such as high specific surface area, high solubility, high dispersion, and small specific gravity compared with the other two crystalline phases.[4] As being reported, precipitation of calcium and carbonate ions in the aqueous solution in the absence of any additives results in the formation of typical rhombohedral calcite crystals.[5] Unlike calcite, vaterite is rarely found in either biological or nonbiological systems.[6] Vaterite transforms easily and irreversibly into thermodynamically stable forms when in contact with water, so it can only be fabricated in the presence of specific additives in a controlled environment. For instance, anionic dendrimers could induce the formation of spherical vaterite particles,[4] and double hydrophilic block copolymers were used in the precipitation of spherical or hollow shell vaterite particles in solution.[7] A water-in-oil system with SDS as the anionic surfactant was used for morphosynthesis of vaterite microsponges.[8] Recently, Tremel and co-workers[9] reported the crystallization of vaterite nanowires by the cooperative interaction of the tailor-made nucleation surface and polyelectrolyte, where nanowire bundles of vaterite were formed through the interaction of a dissolved polyelectrolyte (poly(acrylic acid) Na salt) with a self-assembled organic monolayer. Park et al.[10] reported that hemispherical vaterite was formed selectively at the air/water interface by the mediation of poly(ethyleneimine) dissolved in supersaturated calcium bicarbonate solution. Hosoda et al.[11] showed that vaterite thin films could be formed on crystalline poly(vinyl alcohol) matrixes simply by adding poly(glutamic acid) in solution. In addition, Cho and co-workers[12] reported biomimetic fabrication of vaterite film from amorphous calcium carbonate on polymer melt.

It is well-known that surfactant molecules, above the critical micelle concentration (CMC), dynamically and spontaneously associate to aggregates known as micelles in water.[13] But the aqueous micelles are the most disorganized surfactant assemblies.[14] Recently, there has been a considerable amount of research dealing with the effects of nonaqueous polar solvents, such as glycerol, formamide, and ethylene glycol, on the micellization process.[15,16] Ethylene glycol (EG) is of particular interest in that it has many characteristics similar to those of water. EG molecules are small and can form hydrogen-bonded networks similar in nature to those of water but considerably different in the details of the structure. EG also possesses a high cohesive energy and a fairly high dielectric constant. However, to the best of our knowledge, there have been no reports on the preparation of $CaCO_3$ (vaterite) with various morphologies in the water−EG mixed system.

So far, most of the preparations of $CaCO_3$ were carried out at room temperature; very few reports investigated the influence of temperature on the morphology and crystalline phase of $CaCO_3$. We have found that microwave heating has a great effect on the morphology of $CaCO_3$. The application of microwave heating in synthetic chemistry is a fast-growing area of research.[17,18] Since the first reports of microwave-assisted synthesis in 1986,[19,20] microwave heating has been accepted as a promising method for rapid volumetric heating, which results in higher reaction rates and selectivities, reduction in reaction times often by orders of magnitude, and increasing yields of products compared to conventional heating methods. As a result, this has opened up the possibility of realizing new reactions in a very short time.

Herein we report for the first time microwave-assisted morphosynthesis of $CaCO_3$ (vaterite) in a water/EG system with surfactants. Vaterite with various morphologies has been obtained by controlling the experimental parameters. The self-assembly plays an important role in the formation of these vaterite crystals with various morphologies. The experimental conditions for typical samples and their morphologies are listed in Table 1.

* Corresponding author. E-mail: y.j.zhu@mail.sic.ac.cn. Tel: +86-21-52412616 Fax: +86-21-52413122.

10.1021/jp060939s CCC: $33.50
Published on Web 04/05/2006

TABLE 1: Experimental Conditions for Typical Samples and Their Morphologies[a]

sample	solution	time (min)	morphology
1	SDS (1.5 mmol)/EG (10 mL)/0.75 mol/L $Ca(CH_3COO)_2$ aqueous solution (2 mL) + SDS (1.5 mmol)/EG (10 mL)/0.75 mol/L Na_2CO_3 aqueous solution (2 mL)	8	dagger-like
2	same as sample 1	5	bicone-like
3	same as sample 1	6	dagger-like
4	same as sample 1	7	dagger-like
5	same as sample 1	10	dagger-like
6	same as sample 1	30	irregular
7	EG (10 mL)/0.75 mol/L $Ca(CH_3COO)_2$ aqueous solution (2 mL) + EG (10 mL)/0.75 mol/L Na_2CO_3 aqueous solution (2 mL)	10	irregular
8	SDS (3 mmol)/EG (10 mL)/0.75 mol/L $Ca(CH_3COO)_2$ aqueous solution (2 mL) + SDS (3 mmol)/EG (10 mL)/0.75 mol/L Na_2CO_3 aqueous solution (2 mL)	10	irregular
9	same as sample 8	20	shuttle-like
10	CTAB (1.5 mmol)/EG (10 mL)/0.75 mol/L $Ca(CH_3COO)_2$ aqueous solution (2 mL) + CTAB (1.5 mmol)/EG (10 mL)/0.75 mol/L Na_2CO_3 aqueous solution (2 mL)	10	regular microspheres

[a] All samples were prepared by microwave heating at 100 °C.

Experimental Section

Calcium acetate monohydrate ($Ca(CH_3COO)_2 \cdot H_2O$), sodium carbonate (Na_2CO_3), ethylene glycol (EG), and cetyltrimethylammonium bromide (CTAB) were of analytical grade and sodium dodecyl sulfate (SDS) was chemically pure. All the reagents were purchased and used as-received without further purification. Deionized water was used to prepare aqueous solutions of $Ca(CH_3COO)_2$ and Na_2CO_3. Calcium carbonate ($CaCO_3$) was prepared via the reaction between Na_2CO_3 and $Ca(CH_3COO)_2$ in a mixed solvent of water and EG using SDS as the anionic surfactant by microwave heating. Sample 1 was prepared as follows: solution A was prepared by dissolving 1.5 mmol of SDS in 2 mL of 0.75 mol/L $Ca(CH_3COO)_2$ aqueous solution and 10 mL of EG under magnetic stirring. Solution B was prepared by dissolving 1.5 mmol of SDS in 2 mL of 0.75 mol/L Na_2CO_3 aqueous solution and 10 mL of EG under magnetic stirring. Two solutions were mixed quickly under magnetic stirring at room temperature. The resultant solution quickly became obviously turbid, indicating the formation of $CaCO_3$ nuclei. The suspension was microwave-heated to 100 °C and maintained at 100 °C for 8 min. Then, the microwave heating was terminated and the products were collected by centrifugation, washed with deionized water three times and absolute ethanol three times, and dried at 60 °C in air.

The microwave oven (2.45 GHz, maximum power 300 W) used was a focused single-mode microwave synthesis system (Discover, CEM, USA). The unique, circular single-mode cavity ensured samples were in a homogeneous highly dense microwave field. The system was equipped with an in situ magnetic stirrer and a water-cooled condenser. The temperature was controlled by automatic adjustment of microwave power. X-ray diffraction (XRD) was performed with a Rigaku D/max 2550 V X-ray diffractometer using graphite monochromatized high-intensity Cu Kα radiation (λ = 1.54178 Å). Transmission electron microscopy (TEM) and selected-area electron diffraction (SAED) were recorded on a JEOL JEM-2100F field-emission transmission electron microscope using an accelerating voltage of 200 kV. Scanning electron microscopy (SEM) was recorded on a JSM-6700F field-emission scanning electron microscope (FE-SEM).

Results and Discussion

Figure 1 shows the XRD pattern of sample 1 prepared by the microwave-assisted method in the water/EG/SDS system at 100 °C for 8 min. One can see that the phase of the product was well-crystallized vaterite with a hexagonal structure (JCPDS 33-0268). It has been reported that calcite was formed in the water/SDS system.[21] This indicates that the presence of EG affected the precipitation rate of vaterite and limited its phase transformation into calcite and therefore was favorable for the formation of vaterite.

The morphology of sample 1 was examined by TEM and FE-SEM (Figure 2). The lower magnification TEM (Figure 2a) and FE-SEM micrographs (Figure 2d) of sample 1 show that the morphology of the product was dagger-like. From the high-magnification TEM (Figure 2b) and FE-SEM micrographs (Figure 2e) of sample 1, one can clearly see that each dagger-like structure consisted of ellipsoid-like vaterite nanoparticles. Figure 2c shows a TEM micrograph of an individual dagger-like vaterite structure of sample 1 and its corresponding SAED pattern (the inset). The SAED patterns taken at different spots of the single dagger-like vaterite structure were essentially the same, indicating that the ellipsoid-like vaterite nanoparticles which constituted the dagger-like vaterite structure had the same orientation.

To study the influence of reaction time, we collected products at various times. Figure 3 shows XRD patterns of samples 1−6. Samples 1−5 have similar XRD patterns, which can be indexed

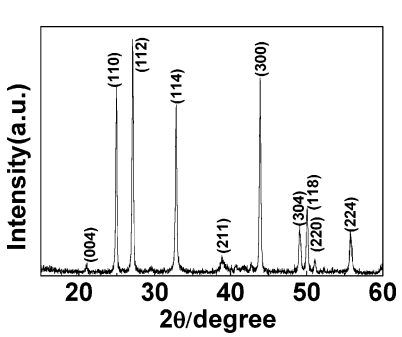

Figure 1. XRD pattern of sample 1.

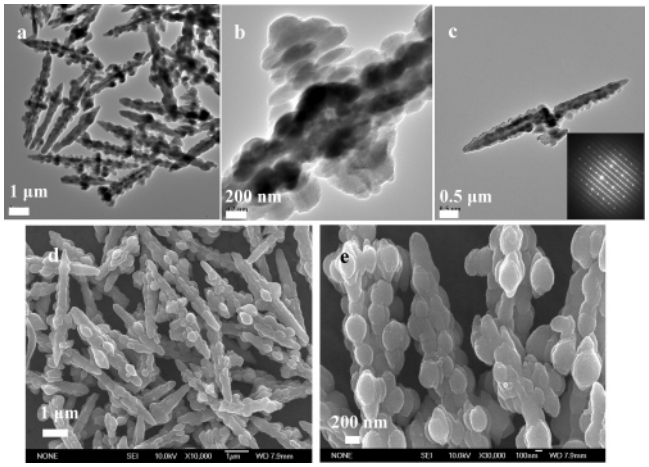

Figure 2. TEM (a−c) and FE-SEM (d and e) micrographs of sample 1.

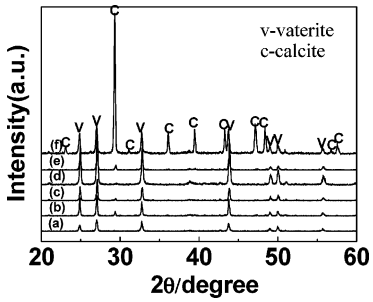

Figure 3. XRD patterns of samples 1−6: (a) sample 2; (b) sample 3; (c) sample 4; (d) sample 1; (e) sample 5; (f) sample 6.

to hexagonal vaterite (JCPDS 33-0268). However, in addition to the main phase of vaterite, samples 3, 4, and 5 had a small quantity of calcite. The main phase of sample 6 was calcite in coexistence with a minority phase of vaterite. This indicates that when the reaction time is prolonged, vaterite, as a less stable polymorph which is stabilized kinetically, will transform into calcite. This is consistent with the phase transformation of $CaCO_3$ via a solvent-mediated process.[3]

The reaction time played an important role in the morphology of vaterite. Figure 4 presents FE-SEM micrographs of samples prepared in the water/EG/SDS system by microwave heating at 100 °C for different reaction times. Bicone-like vaterite structures were obtained when the reaction time was 5 min (sample 2). It is interesting that dagger-like vaterite structures could be obtained when the reaction time was increased to 6 min (sample 3). Similar dagger-like vaterite structures formed for samples prepared for 7 min (sample 4), 8 min (sample 1), or 10 min (sample 5) (Figures 2 and 4). In contrast, dagger-like vaterite structures were not observed by using an oil bath at 100 °C for 10 min instead of microwave heating. A large number of rhombohedral calcite crystals were formed, although some dagger-like vaterite structures were still present when the reaction time was prolonged to 30 min, which was consistent with the main phase of calcite in the XRD pattern (Figure 3f). This implies that phase transformation of vaterite to calcite occurs with increasing the reaction time. We can conclude that the morphology and size of vaterite structures were sensitive to the reaction time.

The effect of SDS on the morphology of vaterite was also studied. With keeping the other conditions the same as sample 5, sample 7 was prepared in the absence of SDS and samples 8 and 9 were prepared with the doubled amount of SDS. The XRD pattern of sample 7 could be indexed to a single phase of

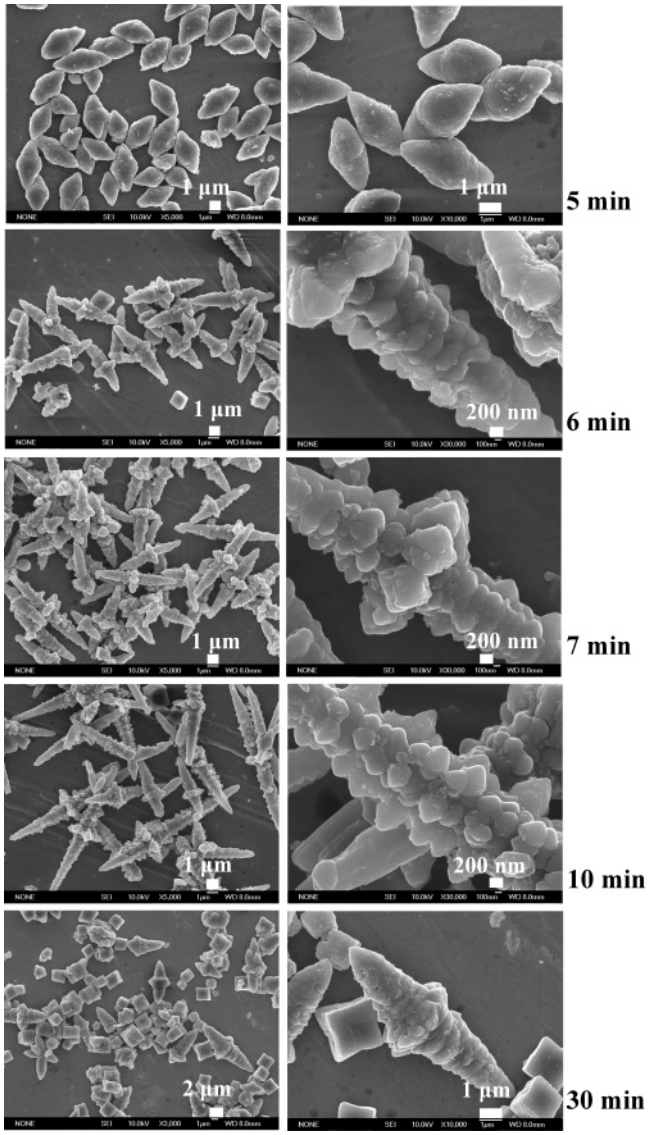

Figure 4. FE-SEM micrographs of samples 2−6. Samples 2, 3, 4, 5, and 6 correspond to the reaction times of 5, 6, 7, 10, and 30 min, respectively.

hexagonal vaterite (JCPDS 33-0268). FE-SEM micrographs of sample 7 (Figure 5a,b) show that the morphology of this product was irregular. The morphology of sample 8 was irregular, too. If the reaction time was prolonged to 20 min (sample 9), a single phase of hexagonal vaterite (JCPDS 33-0268) with a shuttle-like morphology was obtained (Figure 5c,d).

We have also investigated the influence of different surfactants on the morphology of the products. The experiment was carried out under the same conditions as sample 5 but using CTAB instead of SDS (sample 10). Samples 10 consisted mainly of the phase of hexagonal vaterite; a small quantity of calcite was also present. FE-SEM (Figure 6a,b) and TEM (Figure 6c,d) micrographs of sample 10 show monodisperse vaterite microspheres with an average size of $\sim$1 μm. One can see that each vaterite microsphere consists of self-assembled vaterite nanoparticles with diameters of $\sim$50 nm. This implied a multistep growth mechanism where small nanoparticles were first formed, and then microspheres were formed by self-assembly of smaller nanoparticles. The process is strongly coupled with the surface-adsorbed molecules, CTAB.

Next we discuss the formation mechanism of vaterite. One of the critical factors responsible for the shape determination

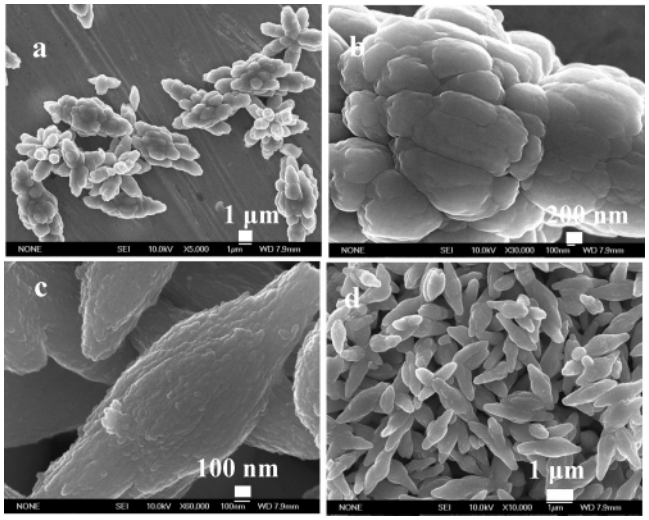

Figure 5. FE-SEM micrographs. (a) and (b) sample 7; (c) and (d) sample 9.

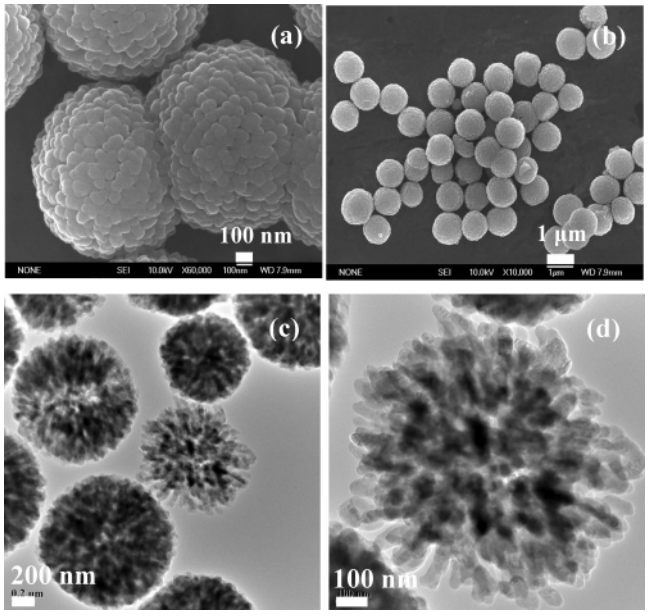

Figure 6. FE-SEM (a and b) and TEM (c and d) micrographs of sample 10.

of the crystals is the crystallographic phase of the initial seed during the nucleation processes.[22] Potentially, the seed can have a variety of different crystallographic phases, but the stable phase is highly dependent on its synthesis environment. We propose that EG in water can stabilize the vaterite nuclei and restrict their transformation to calcite. In addition, SDS polar groups act as active sites for $CaCO_3$ nucleation, due to their electrostatic interaction with calcium ions. Ca^{2+} strongly adsorbed on the micellar surfaces of opposite charge; hence, nucleation occurs at a much faster rate on the surface of SDS micelles than in the bulk of the solution. Microwave heating leads to a high heating rate and a rapid increase in temperature during the nucleation process, which is important for fast nucleation and growth of crystals. The movement and polarization of EG and water molecules under the rapidly changing electric field of the microwave reactor may result in transient, anisotropic microdomains for the reaction system, facilitating the anisotropic growth of $CaCO_3$. On the other hand, the shape of SDS micelles in the water−EG mixed solvents is destroyed and reorganized

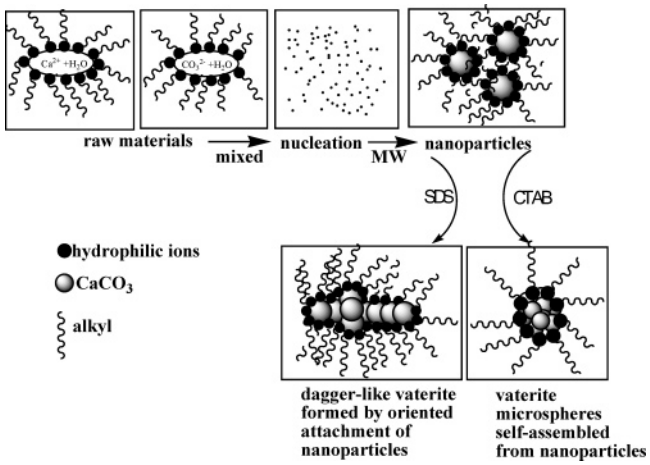

Figure 7. Schematic illustration of the formation process of vaterite with a dagger-like morphology and microspheres assembled from nanoparticles by the microwave-assisted method in water/EG/SDS and water/EG/CTAB systems.

due to the fast increase in temperature. Under the above conditions, the anisotropic ellipsoid-like vaterite nanoparticles are formed.

Reduction in surface energy is the primary driving force for crystal growth and morphology evolution. The formation of dagger-like vaterite structures cannot be explained by the most cited Ostwald ripening process, in which crystal growth is described in terms of growth of larger particles at the expense of smaller particles. It may follow the oriented attachment mechanism proposed and demonstrated in anatase TiO_2 by Penn and Benfield.[23,24] Titania nanoparticles can attach to each other along one crystallographic dimension to produce titania chains under hydrothermal conditions. Nanorods of ZnO have also been made by the oriented attachment of nanocrystals.[25] The oriented attachment mechanism was also suggested for the formation of $CaCO_3$ hexagonal prism crystals.[26] In our case, the formation of dagger-like vaterite structures is realized by the precise, crystallographically controlled attachment of the initially formed ellipsoid-like vaterite nanoparticles.

In the case of CTAB, it is proposed that the shape of the CTAB micelles is spherical and more stable than that of SDS. So spherical vaterite nanoparticles are formed and then self-assembled into microspheres. The formation process of vaterite with a dagger-like morphology and microspheres assembled from nanoparticles by the microwave-assisted method in water/EG/SDS and water/EG/CTAB systems is schematically illustrated in Figure 7. The detailed formation mechanism needs to be further investigated.

Conclusion

In summary, we have developed a fast microwave-assisted method for synthesis of $CaCO_3$ (vaterite) with various morphologies in the water/EG system with surfactants. Our experiments show that microwave heating, reaction time, surfactant, and the water−EG mixed solvents play important roles in the morphology of vaterite. Vaterite with dagger-like, bicone-like, shuttle-like morphology and microspheres self-assembled from nanoparticles have been obtained by adjusting the experimental parameters. We expect that this microwave-assisted method may also be extended to quickly synthesize other kinds of nanostructures with unique morphologies.

Acknowledgment. Financial support from the National Natural Science Foundation of China (50472014) and Chinese

Academy of Sciences under the Program for Recruiting Outstanding Overseas Chinese (Hundred Talents Program) is gratefully acknowledged. We thank the Fund for Innovation Research from Shanghai Institute of Ceramics, Chinese Academy of Sciences.

References and Notes

(1) Lowenstam, H. A. *Science* **1981**, *211*, 1126.
(2) Mann, S. *Nature* **1988**, *332*, 119.
(3) López-Macipe, A.; Gómez-Morales, J.; Rodríguez-Clemente, R. *J. Cryst. Growth* **1996**, *166*, 1015.
(4) Naka, K.; Tanaka, Y.; Chujo, Y. *Langmuir* **2002**, *18*, 3655.
(5) Yu, J.; Zhao, X.; Cheng, B.; Zhang, Q. *J. Solid State Chem.* **2005**, *178*, 861.
(6) Addadi, L.; Aizenberg, J.; Albeck, S.; Fanlini, G.; Weiner, S. *Supramolecular Stereochemistry*; Kluwer Academic Publisher: Dordrecht, The Netherlands, 1995; p 127.
(7) Cölfen, H.; Antonietti, M. *Langmuir* **1998**, *14*, 582.
(8) Walsh, D.; Lebeau, B.; Mann, S. *Adv. Mater.* **1999**, *11*, 324.
(9) Balz, M.; Therese, H. A.; Li, J.; Gutmann, J. S.; Kappl, M.; Nasdala, L.; Hofmeister, W.; Butt, H. J.; Tremel, W. *Adv. Funct. Mater.* **2005**, *15*, 683.
(10) Park, H. K.; Lee, I.; Kim, K. *Chem. Commun.* **2004**, 24.
(11) **(**11**)** Hosoda, N.; Sugawara, A.; Kato, T. *Macromolecules* **2003**, *36*, 6449.
(12) Han, J. T.; Xu, X. R.; Kim, D. H.; Cho, K. *Chem. Mater.* **2005**, *17*, 136.
(13) Fendler, J. H. *Membrane Mimetic Chemistry*; Wiley: New York, 1982.
(14) Fendler, J. H. *Chem. Rev.* **1987**, *87*, 877.
(15) Wärnheim, T. *Curr. Opin. Colloid Interface Sci.* **1997**, *2*, 472.
(16) Zana, R. *Colloids Surf., A* **1997**, *123*−*124*, 27.
(17) Perreux, L.; Loupy, A. *Tetrahedron* **2001**, *57*, 9199.
(18) Namboodiri, V. V.; Varma, R. S. *Green Chem.* **2001**, *3*, 146.
(19) Gedye, R.; Smith, F.; Westaway, K.; Humera, A.; Baldisera, L.; Laberge, L.; Rousell, L. *Tetrahedron Lett.* **1986**, *27*, 279.
(20) Giguere, R.; Bray, T. L.; Duncan, S. M.; Majetich, G. *Tetrahedron Lett.* **1986**, *27*, 4945.
(21) Wei, H.; Shen, Q.; Zhao, Y.; Zhou, Y.; Wang, D. J.; Xu, J. F. *J. Cryst. Growth* **2005**, *279*, 439.
(22) Lee, S. M.; Cho, S. N.; Cheon, J. *Adv. Mater.* **2003**, *15*, 441.
(23) Penn, R. L.; Banfield, J. F. *Geochim. Cosmochim. Acta* **1999**, *63*, 1549.
(24) Penn, R. L.; Banfield, J. F. *Science* **1998**, *281*, 969.
(25) Pacholski, C.; Kornowski, A.; Weller, H. *Angew. Chem., Int. Ed.* **2002**, *41*, 1188.
(26) Zhan, J.; Lin, H.; Mou, C. *Adv. Mater.* **2003**, *15*, 621.